



Report

Optical coherence tomography: feasibility for basic research and image-guided surgery of breast cancer

Stephen A. Boppart¹, Wei Luo², Daniel L. Marks², and Keith W. Singletary³

¹Department of Electrical and Computer Engineering, Bioengineering Program, Beckman Institute for Advanced Science and Technology, College of Medicine; ²Beckman Institute for Advanced Science and Technology; ³Department of Food Science and Human Nutrition, Functional Foods for Health Program, University of Illinois at Urbana-Champaign, Urbana, IL, USA

Key words: breast cancer imaging, image-guided surgery, MNU-induced carcinogenesis, optical coherence tomography, optical imaging, rat mammary tumor

Summary

Diagnostic trends in medicine are being directed toward cellular and molecular processes, where treatment regimens are more amenable for cure. Optical imaging is capable of performing cellular and molecular imaging using the short wavelengths and spectroscopic properties of light. Diffuse optical tomography is an optical imaging technique that has been pursued as an alternative to X-ray mammography. While this technique permits non-invasive optical imaging of the whole breast, to date it is incapable of resolving features at the cellular level. Optical coherence tomography (OCT) is an emerging high-resolution biomedical imaging technology that for larger and undifferentiated cells can perform cellular-level imaging at the expense of imaging depth. OCT performs optical ranging in tissue and is analogous to ultrasound except reflections of near-infrared light are detected rather than sound. In this paper, an overview of the OCT technology is provided, followed by images demonstrating the feasibility of using OCT to image cellular features indicative of breast cancer. OCT images of a well-established carcinogen-induced rat mammary tumor model were acquired. Images from this common experimental model show strong correlation with corresponding histopathology. These results illustrate the potential of OCT for a wide range of basic research studies and for intra-operative image-guidance to identify foci of tumor cells within surgical margins during the surgical treatment of breast cancer.

Introduction

Breast cancer continues to have a significant impact on the lives of every individual in the United States and throughout the world. According to 2003 cancer statistics from the American Cancer Society, an estimated 211,300 new cases of invasive breast cancer and 55,700 new cases of *in situ* breast cancer are expected to occur in the US this year, being the most frequently diagnosed non-skin cancer in women [1, 2]. Breast cancer ranks second among cancer deaths in women (second to lung cancer) with an estimated 40,200 deaths anticipated in 2003 [1, 2]. Many controversies remain in the treatment of breast cancer, particularly for ductal carcinoma *in situ* (DCIS). It is not clear

if and when DCIS will progress and therefore what type of treatment regime, if any, is appropriate. Because early stage DCIS and other breast malignancies are often difficult to detect and track using mammograms, high-resolution imaging modalities may play a role in elucidating the fundamental mechanisms of the disease and its response to therapy.

As with all malignancies, early detection and treatment results in a more favorable prognosis. As one indicator of success, the 5-year relative survival rate for localized breast cancer is now at 97%, compared to only 72% in the 1940s [2]. Unfortunately, following loco-regional metastasis, the 5-year survival rate falls to 78% and for distant metastasis, the rate is only 23%. After 5 years, survival following the diagnosis of

breast cancer continues to fall for all stages [2]. This data indicates that our current detection methods and treatment protocols must still be improved.

Light in the near-infrared region of wavelengths is capable of propagating deeply through biological tissue. A 'biological window' exists in this wavelength region where attenuation is governed by scattering rather than absorption [3]. For this reason, and as an alternative to X-ray mammography that uses ionizing radiation, optical mammography is being developed. Spatial maps (images) of tumors and contrast-agent-tagged sites have successfully been imaged using diffuse optical tomography (DOT) [4–6]. Unfortunately, because photons undergo multiple random scattering events as they propagate through highly-scattering tissue such as breast, spatial information and imaging resolution is lost. DOT can localize relatively large (~1 cm) tumors deep in breast tissue, but resolutions on the order of several millimeters do not permit imaging of small early-stage tumors and cellular-level resolution is not possible [4–6]. An inherent trade-off between depth of imaging and resolution exists in many imaging modalities, including optics. Therefore, since optical techniques are capable of imaging tissue at cellular resolutions, in certain invasive scenarios, such as fine-needle aspirations, core-needle biopsies, or surgical resections, one could take advantage of high-resolution imaging and forego the non-invasive advantage of DOT.

Optical coherence tomography (OCT) is an emerging high-resolution imaging technology that commonly uses near-infrared wavelengths to perform optical ranging in an analogous manner to ultrasound imaging [7–9]. While depth of imaging is limited to only a few millimeters in highly-scattering tissues, imaging resolutions less than 1 micron have been demonstrated [10]. With these high resolutions, OCT performs an 'optical biopsy', capturing images that approach the resolution and represent the architectural morphology commonly found in histology [11–13]. While histology is based on thin slices of tissue that are selectively stained to highlight selected features and viewed by transmitting light through the slices, OCT generates cross-sectional images representing the spatially-localized intensity of optical backscatter of light passed through tissue from above, typically without the addition of exogenous stains or probes. Remarkably, the stained morphological features in histology correspond well with the backscattering features detected in OCT, even though the light propagation through the tissue for each technique is

in orthogonal directions. The use of OCT could therefore be a powerful alternative to standard histological processing in the investigation and treatment of breast cancer. OCT could be used to rapidly scan large areas of tissue for suspicious breast architecture or morphology, to guide at the cellular level the surgical resection of neoplastic disease, and to scan tumor margins for the presence of residual disease, tumor foci, and potentially even metastasizing tumor cells.

High-resolution optical imaging is performed at the expense of limited imaging penetration. However, there are numerous experimental and surgical scenarios where it is feasible to deliver the imaging beam close to the tissue of interest for high-resolution imaging. OCT imaging can be performed through small needles and hand-held probes [14, 15]. Non-optical devices are currently used for fine-needle aspirations and core-needle biopsies of breast masses, and in the open surgical field. Modifying these devices to integrate imaging optics is an engineering problem that can be readily addressed. In this paper, we demonstrate the feasibility of OCT for imaging breast cancer. We use a well-characterized carcinogen-induced rat mammary tumor model and compare OCT images with corresponding light microscopy observations of histological sections. To date, OCT has not been applied to imaging breast cancer. In part, this may be because OCT imaging of breast parenchyma and cancer is only feasible through invasive procedures. However, because of the prevalence of this disease and its impact on our lives, new technologies that have the potential to improve diagnosis and surgical treatment must be fully investigated. In addition, because breast cancer is a molecular disease that has early-stage cellular changes, technologies that can detect changes at the cellular level may be more amenable for the detection and treatment of this disease.

Surgical treatment of breast cancer

The importance of high-resolution imaging in breast cancer cannot be overemphasized. Intra-operative image-guided interventions in breast cancer surgery may ascertain the local extension of the disease, whether breast tissue surrounding the tumor is tumor-free or contains tumor cells (occult disease). The extent of local extension and tumor cell infiltration in the surrounding breast parenchyma has been investigated in a group of 264 mastectomy specimens [16]. Results indicate that 41% of the patients had additional foci 2 cm or further from the primary

tumor, and 11% had additional foci 4 cm or further from the primary tumor [16]. Of these, the additional foci were intra-ductal in two-thirds of the patients. These observations have been confirmed in a more recent investigation [17]. Approximately 40–50% of all solid tumors develop local or loco-regional recurrence following optimum, surgical and/or radiation therapy. These findings validate that local or loco-regional recurrence of solid tumors following radical resection and/or radiation therapy remains a significant problem. The major reason for this failure rate is because, during the time of initial therapy, adequate margins of normal surrounding tissue are either not resected or included in the portals of radiation therapy. The single most important reason for this failure to obtain adequate margins is the lack of well-developed technology that can distinguish with a reasonable degree of confidence that the presumed margin of normal tissue surrounding the tumors is indeed normal, and that there are no nests of occult cancer within these tissues. Recently, with the increasing use of ultrasound and MRI, diagnostic accuracy of the extent of local spread of a given tumor has improved considerably. Nevertheless, both these techniques are unable to provide information on the extent of microscopic spread of malignant cells at the periphery of a solid tumor. This automatically leads the clinician frequently to under-stage the disease, which in turn impairs the ability not only to adequately treat, but also to properly prognosticate.

Attempts are being made to design novel techniques to identify tissues infiltrated with tumor. One method being used is radio-guided surgery [18]. The general principle is to radio-label a cancer-specific monoclonal antibody (MAB) and inject this MAB into the tumor prior to surgery. Then, during surgery, a handheld counter is used to define the tumor and the tumor margins (which show radioactivity) to be resected. Although this is an attractive premise, unfortunately it is not possible to prepare MABs for all solid tumors. Secondly, most MABs are hybrids of mouse proteins. Thus, foreign protein allergy can be a limiting factor. Furthermore, the accuracy of detecting cancerous tissues is not as efficient as was originally presumed. Therefore, it is imperative that the search be continued and perfected for non- or minimally-invasive technologies such as OCT.

The open-surgical-field resection of tumors is frequently guided by viewing CT or MRI films of the tumor that were acquired prior to surgery. These static images are frequently viewed by the surgeon prior

to and during the operation. However, registration is often performed by identifying anatomical landmarks in both the images and the tissue during the procedure. Advanced image-guided interventional procedures have developed methods to overlay and register the images with the tissue in real-time, providing the surgeon with a 'virtual' image of the tumor referenced to the physical anatomy [19]. The current practice in surgical oncology is to excise the primary tumor with an 'arbitrary margin' of presumed normal tissue and send the specimen to the pathologist to assess whether the margins of excision are clear. Even if the margins are presumed to be free of occult disease, still the practice is to radiate the entire breast. The objective is to eradicate any undetected occult disease, either an extension of the primary cancer or multi-centric regions.

Aside from being a time- and labor-intensive process involving a fully-staffed operating room and pathology laboratory, not infrequently this process is laden with sampling errors. Thus, the extent of occult disease left behind following a meticulous lumpectomy is still an open question and is one factor, for instance, contributing to the central dogma for a T₁–T₂ primary breast cancer of radiating all patients who had a lumpectomy. It is common practice, therefore, to take wide surgical margins in an effort to resect the small regions of tissue or the few remaining tumor cells that have migrated away from the central tumor, at the expense of large volumes of normal tissue. While this may be without complication for particular tumors and for specific tumor sites, it is detrimental for tumors located in the brain or other sensitive and functional regions of the body where the surgical removal of normal tissue must be minimized. It would be advantageous to have an image-guided interventional system capable of scanning both the resected tissue and the walls of the tumor cavity for neoplastic tissue or cells in real-time and at cellular resolutions.

The management of ductal carcinoma *in situ* (DCIS) is a primary example where OCT may have a significant impact. DCIS is a proliferation of presumably malignant epithelial cells confined to the mammary ducts and lobules without demonstrable evidence of invasion through the basement membrane into the surrounding stroma. The incidence of DCIS has increased considerably since 1983. Most likely, screening mammography has increased the awareness of microcalcifications in mammograms, which has increased needle localization biopsies with histological diagnoses of DCIS. The ability to identify small clusters of tumor cells close to the intra-ductal foci as

evidence of ‘minimal’ stromal invasion is quite difficult, primarily due to sampling errors. Thus, even after a biopsy of a presumed site of DCIS, the question remains how best to identify the probable sites of invasion of the surrounding mammary parenchyma. To complicate the issue, DCIS has been considered by some to be a multi-centric process with separate areas of involved ducts. All of these situations have made the management of DCIS one of the most controversial topics in breast disease. The use of a high-resolution intra-operative image-guidance system using OCT may have the potential to identify small clusters of tumor cells that have invaded the mammary parenchyma.

Optical coherence tomography

Optical coherence tomography is a rapidly emerging high-resolution medical and biological imaging technology [7–9, 11, 12]. OCT is the optical analogue to ultrasound B-mode imaging except reflections of low-coherence light are detected rather than sound. For medical imaging, OCT is attractive because it permits the imaging of tissue microstructure *in situ*, yielding micron-scale resolution images without the need for excision and histological processing. Much of the OCT technology leverages the hardware developed for the telecommunications industry, making the instrument potentially compact and portable (Figure 1).

OCT was originally demonstrated in ophthalmology and has been successfully commercialized for clinical eye examination [20]. Recently, OCT has been applied for imaging a wide range of non-transparent tissues [21–23]. In these tissues, a ‘biological window’ exists where absorption of near-infrared wavelengths is minimal and light can penetrate deep into tissue [3]. In most highly-scattering (non-transparent) tissues, imaging depths of 2–3 mm can be achieved. Imaging studies have been performed in cardiology, gastroenterology, urology, and neurosurgery, among many others [13, 23–25]. High-resolution OCT using short coherence length light sources has achieved axial resolutions of less than 2 μm [10, 26, 27]. High-speed OCT at real-time image acquisition rates has also been demonstrated [28]. OCT has been extended to perform Doppler imaging of blood flow and birefringence imaging to investigate laser intervention [29–31]. Imaging delivery systems have been engineered to enable OCT of external and internal tissues, including microscopes, hand-held probes, imaging needles, catheters,

and endoscopes (Figure 2) [14, 15, 32, 33]. Most recently, OCT has been combined with endoscope-based delivery to perform *in vivo* imaging in human patients [12, 34–37]. *In situ* OCT at near-histological resolution has been used to image morphological differences between normal and neoplastic tissue. OCT images of *in vitro* neoplasms of the brain [13], female reproductive tract [38], the gastrointestinal tract [39], and the bladder [40] have been investigated. High-resolution imaging has permitted real-time tracking of biological development and cell dynamics in living specimens including mesenchymal cell mitosis and neural crest cell migration [41–43]. The high-resolution capabilities for imaging large and undifferentiated cells suggest that OCT could be used to diagnose and monitor early neoplastic changes in humans.

Initial studies have been performed to demonstrate the potential for OCT in a surgical setting. OCT has been used to image surgically-relevant tissues *in vitro* [9, 44–47]. High-speed OCT has been used to track dynamic interventional processes such as laser [45] and radiofrequency [47] ablation as would be performed in a surgical setting. OCT has been used to guide microsurgical procedures such as the repair of nerves and vessels [9]. The majority of studies have suggested that OCT can be used to image both *in vitro* and *in vivo* tissues to identify regions that suggest abnormalities and should be biopsied for histopathological examination. To our knowledge, no studies have been published that demonstrate the use of OCT in breast cancer.

OCT utilizes a technique known as low-coherence interferometry (Figure 1). Measurements are performed using a fiber-optic interferometer with a low-coherence-length light source. Low-coherence light can be generated by a superluminescent diode or an ultrafast (titanium:sapphire) laser. The sample arm of the interferometer contains a modular beam delivery instrument that directs the light onto the tissue and collects the reflected signal. Because OCT can be fiber-optic-based, the imaging beam can be delivered to the tissue and the reflections collected from the tissue using a single optical fiber (approximately 125 μm in diameter). Therefore, imaging can be performed using a scanned optical beam from a surgical microscope or a hand-held probe in the open surgical field or with minimally-invasive needle biopsy probes (Figure 2). The reference arm of the interferometer includes a mechanism for varying the optical path-lengths between the two arms. Optical interference occurs only when the optical distance traveled by the

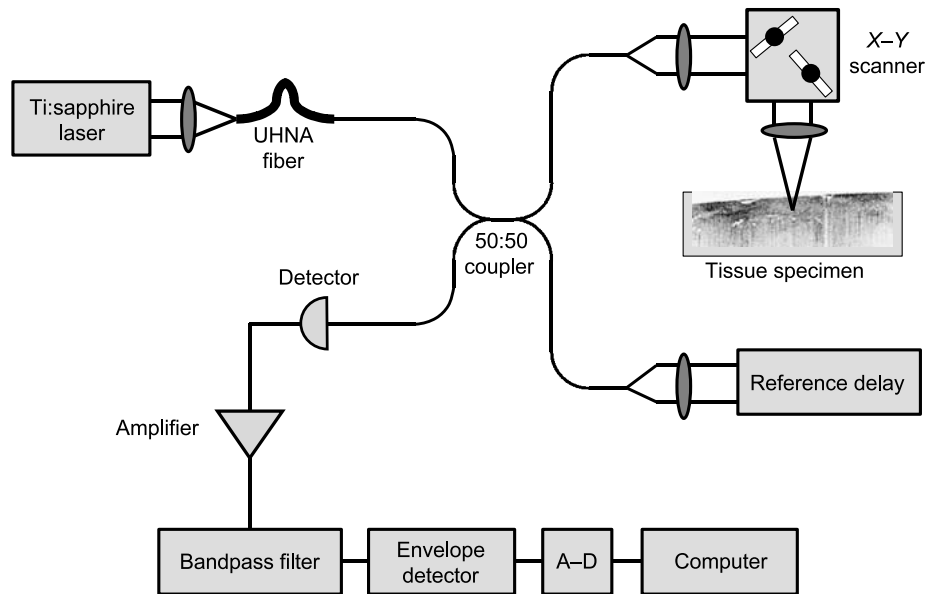


Figure 1. OCT schematic. The OCT technology can be fiber-optic-based, enabling a compact and portable system for use in research, clinical, and surgical settings. Abbreviations: A-D, analog-to-digital converter; UHNA, ultra-high-numerical aperture.

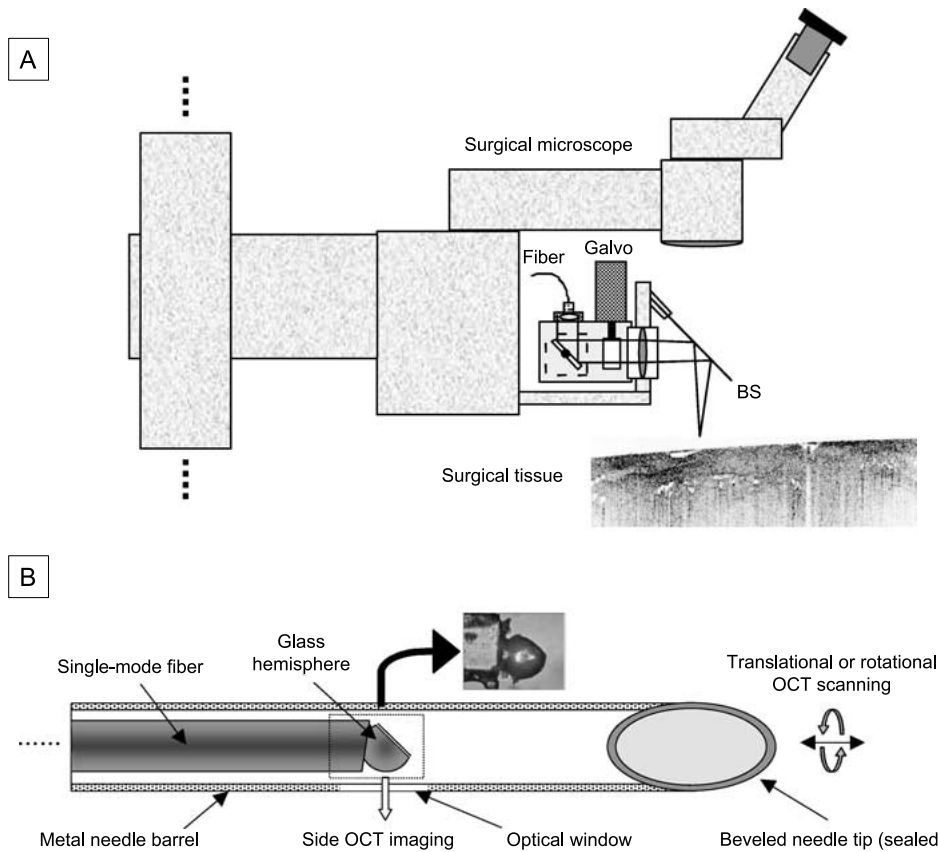


Figure 2. Beam-delivery systems for OCT. The OCT imaging beam can be passed through a number of existing or modified optical instruments including (A) surgical or research microscopes, and (B) fine-needle aspiration and core-needle biopsy probes, among others. Abbreviations: BS, dichroic beamsplitter; Galvo, galvanometer scanner.

light in the tissue sample and reference paths match to within the coherence length of the light source. Image generation is performed by a computer and data is stored digitally. The OCT technology can be made compact and portable, enabling its use on the research laboratory bench, the outpatient service for guided fine-needle aspirations and core-needle biopsies, and in the surgical suite.

Breast cancer research model

The induction of mammary tumors by injection of virgin female rats with the direct-acting carcinogen *N*-methyl-*N*-nitrosourea (MNU) is the most widely-used animal model for studying breast cancer development. Mammary carcinogenesis in this model mimics numerous characteristics associated with human breast carcinogenesis, such as hormone dependency, with histological classifications as adenocarcinomas or papillary carcinomas. The carcinomas induced are locally invasive and can metastasize to liver, lung and spleen [48–53]. It has been reported that MNU-induced palpable tumors are monoclonal in origin, exhibit malignant activation of the *Ha-ras-1* locus, and overexpress several cancer markers. Also, the carcinogen administration protocol can be modified as far as amount and timing of dose of this mammary carcinogen so that the development and histopathology of pre-malignant and malignant lesions, the cellular kinetics of target cells, and detailed characteristics of tumor angiogenesis can be assessed [54–64]. This has led to this model being widely used in chemoprevention studies for breast cancer [65, 66]. Because of the widespread use of this animal model, we have chosen it to demonstrate the ability of OCT to visualize tumor morphology. In particular, this model emulates the pathogenesis of ductal disease found in human DCIS [67]. Because of the existing dogmas associated with this disease, this model and OCT may be particularly well-suited for investigational studies. The use of OCT in this model will permit future tumorigenesis studies investigating the appearance from pre-malignant to metastatic stages and for the chemotherapeutic and surgical treatments of this disease [68–70].

Materials and methods

Tumor induction

Female Sprague–Dawley rats (Harlan Sprague–Dawley, Indianapolis, IN) were housed individually

in rooms with controlled temperature and lighting and fed rodent laboratory chow (Harlan Teklad, Madison, WI). At 55 days of age, six rats were administered one dose of MNU (Sigma Chemical, St. Louis, MO; i.p. 50 mg/kg in saline). Two rats were injected with an equal volume of saline vehicle only. Beginning 3 weeks post-MNU, animals were palpated weekly. Rats that developed palpable mammary masses and normal controls were euthanized by carbon dioxide asphyxiation prior to OCT imaging. Lateral abdominal incisions were made in the abdominal skin to reflect back the abdominal wall, exposing the mammary tissue. Tumors were confirmed visually when the mammary glands were surgically exposed. Animals were positioned on the OCT stage for imaging. All eight animals were imaged for this study, and an average of 20 sites on the mammary gland were imaged for each animal. All animals used in this study were cared for and maintained under protocols approved by the Institutional Animal Care and Use Committee of the University of Illinois at Urbana-Champaign.

Optical coherence tomography

Three-dimensional OCT imaging was performed using a neodymium:vanadate diode-pumped titanium:sapphire laser as a low-coherence light source (Figure 1). Laser output wavelength was centered at 800 nm with a 20 nm bandwidth and consisted of approximately 80 fs pulses at a repetition rate of 80 MHz and an average output power of 500 mW. To spectrally broaden the light and improve axial imaging resolution, the laser output was coupled into a segment of ultrahigh numerical aperture fiber to obtain an axial resolution of 2 μ m [71]. This fiber was fused to a fiber-optic coupler which served as a beam splitter in this fiber-optic-based system. The sample arm light from the fiber was collimated, reflected off a pair of orthogonal galvanometer-mounted mirrors that directed the *X–Y* position of the beam on the tissue, and was focused by a 20 mm focal length achromatic lens to a spot size diameter (transverse resolution) of 10 μ m. Incident optical power on the tissue was measured to be 15 mW. The reference arm contained a galvanometer-mounted retroreflecting mirror translated over an optical pathlength of 3 mm at a frequency of 30 Hz. Reflections from each arm were combined in the fiber-optic coupler and sent to a photodiode. The electrical output of the photodiode was bandpass-filtered, amplified, and digitized with 12-bit accuracy. Custom software assembled digital data for display as

two- or three-dimensional images. Two-dimensional images (512×512 pixels) were acquired in 17 s and three-dimensional data sets consisting of 60 2-D images required 17 min. Faster acquisition rates are feasible ($125 \mu\text{s}$ per image, 7.5 s per 3-D data set) [11, 72] at the expense of lower signal-to-noise ratios. Custom image-processing software algorithms were applied to enhance the visualization of cellular and sub-cellular features [73].

Tissue and image analysis

During OCT imaging, approximately five tissue sites per animal that produced unique features in the OCT images were marked with India ink for registration with histology. The corresponding mammary tumor and surrounding tissue were embedded in tissue freezing medium (Triangle Bio-medical Sciences, Durham, NC, USA) and sectioned with a cryostat (Leica CM3050 S, Leica Microsystems Nussloch GmbH, Germany). Multiple $30 \mu\text{m}$ thick sections were acquired from each side of the India ink-marked plane that corresponded to the OCT imaging plane. Thick sections were obtained to preserve the fine architectural features present in the adipose tissue for correlation with features observed in the OCT images. Sections were stained with hematoxylin and eosin and prepared on glass slides according to standard protocol for light-microscopy observation. Light microscopy was performed using an Olympus BH-2 microscope and digital images were captured (Spot RT Slider, Diagnostic Instruments). Comparisons were made between OCT and light microscopy images, correlating microstructural features. The OCT and histological images presented represent the best match based on the observed architectural morphology.

Three-dimensional data sets were viewed and analyzed using public-domain freeware (ImageJ, National Institutes of Health) on a personal computer. Three-dimensional projections were generated and rotated along X - Y - Z coordinates for visualization of tumors and microstructural features.

Results

Two- and three-dimensional OCT image were acquired from normal mammary tissue and *N*-methyl-*N*-nitrosoureas (MNU)-induced mammary tumors in the rat animal model. Images were acquired to illustrate

architectural morphology at all size scales including solid tumors, early neoplastic changes in ductal morphology, and cellular features near tumor margins.

OCT images and corresponding histology of normal mammary gland tissue and a large MNU-induced tumor are shown in Figure 3. A large portion of breast tissue is composed of fat (adipocytes) which are large lipid-filled cells that provide local homogeneous, low-scattering regions. Adipocytes are most evident in the images of normal mammary tissue (Figure 3(A) and (B)). The collection of adipocytes shown lies beneath a more dense and highly-scattering stroma. Heterogeneous regions are commonly observed, such as in the lower left corner of Figure 3(A). Scattered throughout the OCT images are small highly-scattering (dark) spots that likely represent individual nuclei in both the adipocytes and the stromal cells. The low-scattering regions of adipocytes are in sharp contrast to the dense, highly-scattering collections of tumor cells forming glandular structures or solid tumor masses. As evident in Figure 3, this late-stage mammary tumor can be identified by these dark, highly-scattering regions, which typically correspond to areas with a high-density of tumor cells containing larger, highly-scattering nuclei. The solid tumor identified in Figure 3(C) and (D) has a cell density and optical scattering property close to that of the overlying stroma, making these regions appear similar in the OCT image. However, because tumors are often heterogeneous on a more macro-scale, with varying cell densities, abnormal glandular features, increased vasculature, and disrupted architectural morphology, identification of tumor from normal tissue is possible using these differences. In Figure 3(C), the optical backscatter from the tumor appears more heterogeneous compared to the more homogeneously-backscattering stroma.

Figure 4 shows OCT and histological images of normal and abnormal ducts in this animal tumor model. Normal ducts (Figure 4(A) and (B)) are identified as small thin-walled, circular-appearing structures (Figure 4(A), arrows) if the ducts were imaged in cross-section. Thicker more highly scattering ductal epithelium (Figure 4(C) and (D)) is present in the tumor model compared to the normal control, appearing as larger strongly-scattering regions on OCT and as larger linear collections of dense tumor cells on histology when the ducts are viewed in longitudinal sections (Figure 4(C) and (D)). The ductal origin of this carcinogen-induced tumor and the ability of OCT to detect early neoplastic changes associated with changes in ductal morphology suggest that

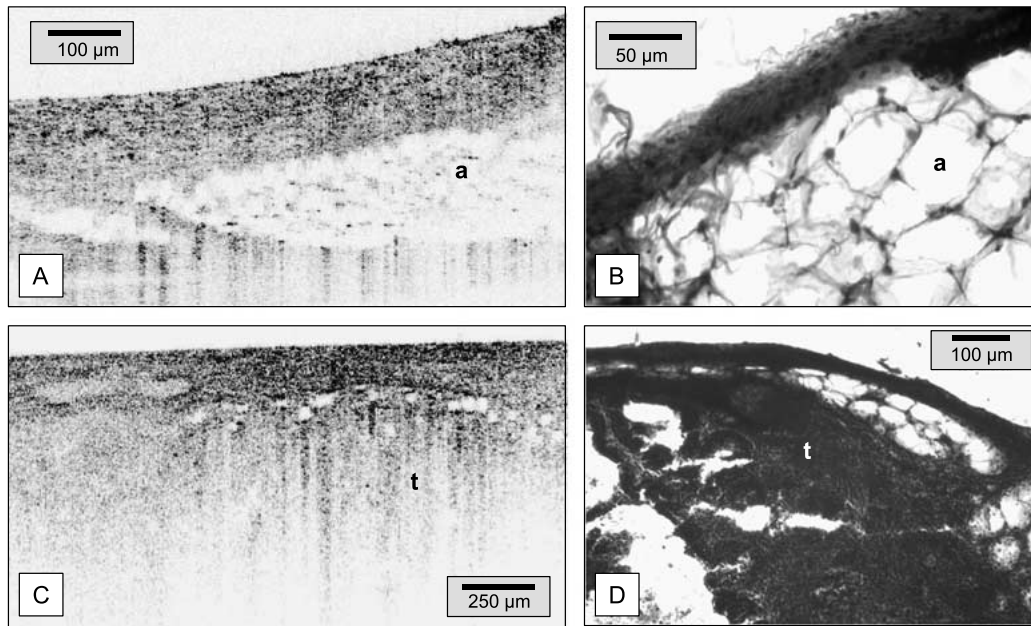


Figure 3. OCT of a late-stage tumor. Images of (A) normal and (C) MNU-induced tumor infiltrated rat mammary tissue with (B) and (D) corresponding light microscopy histopathology. The dense, high-scattering tumor (t) is readily differentiated from the surrounding fatty parenchyma containing adipocytes (a).

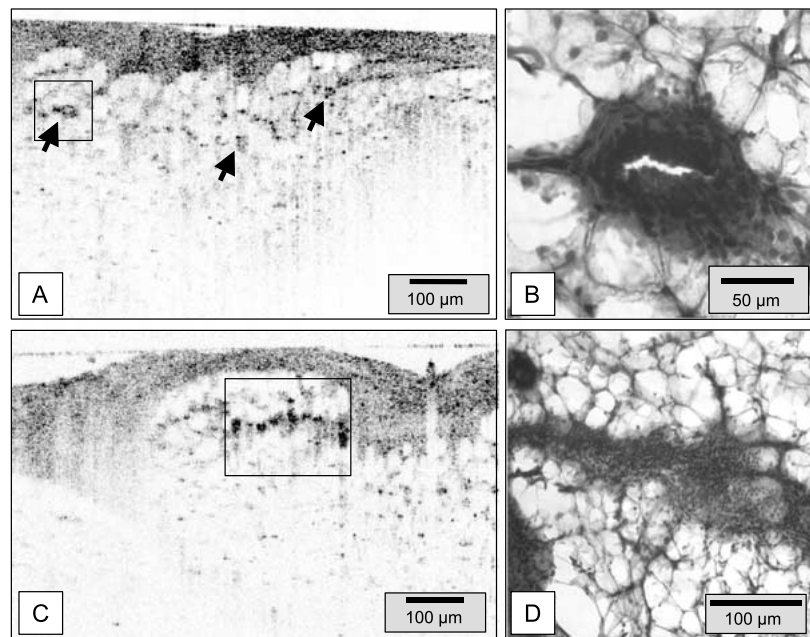


Figure 4. OCT of microscopic early-stage cancer. Images of (A) normal and (C) MNU-induced early stage changes in the ductal epithelium with (B) and (D) corresponding light microscopy histopathology. Early-stage changes are evident by increased optical backscatter from the higher nuclear-to-cytoplasmic ratio and the number of cells surrounding the ducts. Arrows in (A) indicate normal ducts imaged in cross-section and showing thin walls and patent lumens. Boxed regions in (A) and (C) indicate regions of interest for corresponding histology.

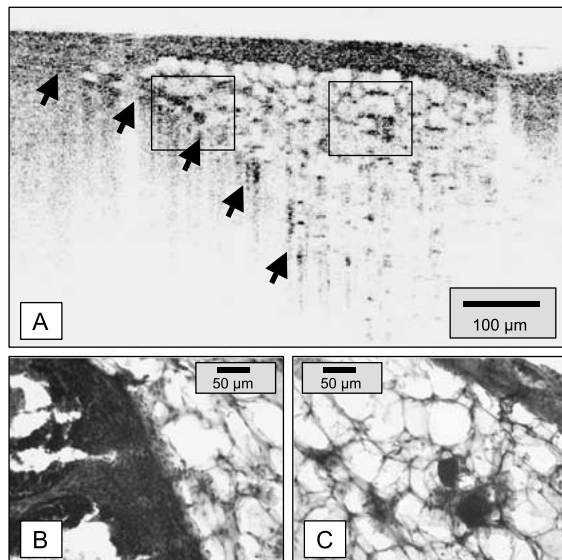


Figure 5. OCT of cellular features along tumor margin. (A) OCT image of a tumor margin with (B) and (C) corresponding histopathology. Cells adjacent to the tumor margin (right box in (A), histology in (C)) appear to be metastatic and in the process of migrating into normal gland parenchyma. Large nuclei, high nuclear-to-cytoplasmic ratio, and increased density of tumor cells contribute to increased optical scattering in OCT images.

OCT may be able to detect early changes prior to solid tumor formation. However, additional studies involving larger numbers of specimens at varying stages of tumorigenesis is required.

The tumor margin is of primary interest in tumorigenesis, metastatic processes, and surgical resection. Figure 5 shows OCT and histological images of a tumor margin (arrows) where individual cells can be observed. Suspect individual cells (Figure 5(A) box, 5(C)) adjacent to the solid tumor show evidence of increased scattering, compared to the surrounding adipocytes. Increased scattering is likely due to the higher nuclear-to-cytoplasmic ratio in these cells and the higher regional cell density. Detection of these cells among relatively low-scattering adipocytes demonstrates the feasibility of detecting these migrating metastatic cells intra-operatively. Detection of individual tumor cells in dense, highly-scattering normal tissue remains problematic for OCT, as frequently is true for histopathology. In this scenario, the addition of an exogenous contrast agent for OCT [74] could help identify tumor cells.

Finally, localizing sub-surface tumors and tumor margins within a three-dimensional tissue volume is facilitated with 3-D OCT image acquisition. Figure 6 shows reconstructed 3-D projections of OCT data sets

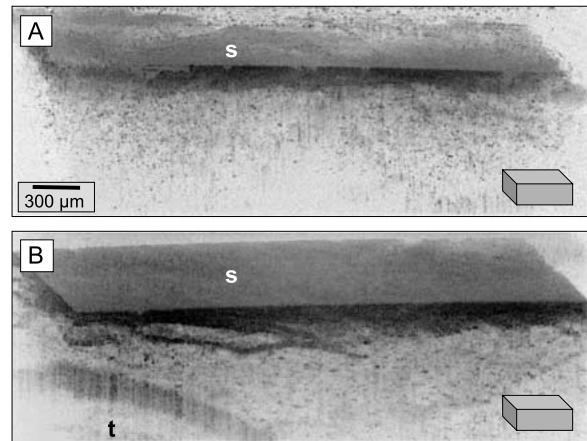


Figure 6. Three-dimensional OCT. Projections of 3-D OCT data sets acquired from (A) normal mammary and (B) MNU-induced tumor tissue are shown. A series of 60 images were acquired and assembled for each projection. Projection orientation is shown by the cube in the lower right corner. A tumor (t) and margin is shown in (B) below the tissue surface (s). Manipulation of these data sets in 3-D space with computer-sectioning at arbitrary planes will permit visualization of cellular features, enabling high-resolution intra-operative surgical guidance and intervention at the cellular level.

acquired from normal and MNU-exposed mammary tissue. These data sets each consist of a series of 60 2-D OCT images acquired at 50 μm inter-slice spacing. The margin of a sub-surface later-stage tumor is evident in the lower-left corner of Figure 6(B). Rotation of these projections and computer-based sectioning along arbitrary axes can be performed to identify suspect regions at high resolutions in large tissue volumes.

Discussion

To date, no published reports have demonstrated the use of OCT for imaging breast cancer. Based on our results presented here, breast cancers can be readily identified *in vitro* in this commonly used rat mammary tumor model. These results, and those from previous OCT studies in other tissue types, suggest the potential of OCT for identifying breast cancers *in vivo*. A large portion of breast parenchyma is composed of fat (adipocytes). These large lipid-filled cells provide local homogeneous, low-scattering regions that distinctly contrast the dense collections of tumor cells forming glandular structures, or for individual cells that have large nuclear-to-cytoplasmic ratios compared to adipocytes. The imaging resolutions used in this study (2 μm axial, 10 μm transverse), and by

many other groups, enable the visualization of larger cells such as adipocytes and undifferentiated cells, which typically range 20–40 microns in size. In these larger cells, cell nuclei and occasionally organelles can be visualized. To date however, challenges remain for visualizing smaller, terminally differentiated cells that are closely packed in highly-scattering tissue. Despite the use of OCT systems with sub-micron resolutions [10], visualization of small (10–15 μm diameter) cells is still problematic, possibly due to complicated optical scattering and coherent speckle artifacts from cellular structures and organelles. Just as molecular imaging techniques are being developed for many clinical modalities such as PET, CT, MRI, and ultrasound, the ability to design and target contrast agents with molecular specificity enables molecular imaging using optical techniques, including OCT [73]. The ability to clearly differentiate normal from abnormal breast tissue at the cellular or molecular level using OCT will be advantageous for both the basic research and surgical treatment of breast cancer.

Surgical intervention is the process of interfering with disease pathogenesis by surgically modifying its course. The use of OCT in an interventional procedure was first demonstrated by the OCT image-guided placement and assessment of retinal laser lesions in the *in vivo* primate eye [75, 76]. These studies examined the dynamic evolution of retinal lesions from continuous wave lasers, and from nanosecond, picosecond, and femtosecond pulses at visible wavelengths (514–580 nm). Although images were acquired every 5 s, the time evolution of lesion morphology enabled a better understanding of the mechanisms of damage. Faster image acquisition rates (4–8 fps) now enable rapid microstructural changes to be observed sequentially over time [30, 40, 47].

The feasibility of OCT to perform high-speed image-guided surgical interventions in highly-scattering tissue has been investigated [45, 47]. The imaging capabilities of OCT have been used to guide and assess the progress of surgical interventions using high-power argon laser ablation and radio-frequency (RF) ablation. In this study, we have demonstrated the use of OCT for imaging tumor morphology in a well-characterized MNU-induced rat mammary tumor model. This model is successfully used in basic science investigations because of its similarities to human breast cancer. Based on strong correlations between OCT and histopathological findings, OCT can accurately image the architectural morphology of breast tumors at multiple scales including large solid tumors,

early-stage ductal changes, and individual tumor cells migrating from tumor margins into surrounding normal adipose tissue. These results suggest that OCT can be used not only for basic science research using this animal model, but also for intra-operative surgical diagnostics.

While the imaging resolutions of this technique surpass those of any other major clinical imaging modality, the relatively shallow imaging depth prevents this technology from being used non-invasively. In this study, a titanium:sapphire laser was used to generate low-coherence light centered at 800 nm wavelength. Because light at longer wavelengths is scattered less in biological tissue, the use of 1300 nm light (a second commonly-used OCT wavelength) is likely to increase imaging depths by a factor of 2–3 [23]. However, the shorter 800 nm wavelength light can provide higher imaging resolution.

Imaging penetration depths, regardless of the OCT wavelength used, do not permit imaging through the full skin thickness and into breast parenchyma. Still, there are many novel scenarios where OCT can make a significant impact in the research and treatment of breast cancer. First, OCT can be used to rapidly scan large areas of tissue, such as the exposed rat mammary fat pad, for suspicious areas of tumor growth, eliminating the need for extensive histological processing of large tissue blocks. Second, the OCT beam can be delivered minimally-invasively through needles commonly used in fine-needle aspirations or core-needle biopsies [14]. OCT can be used for image-guidance to direct the investigator or physician to suspicious areas prior to aspiration or biopsy with the potential to reduce the problems associated with sampling errors and non-diagnostic specimens. OCT image-guided fine-needle aspirations and core-needle biopsies can be used in both basic research studies in anesthetized rats or in clinical human studies and diagnostic procedures. Third, OCT can be performed using a hand-held surgical probe in an open surgical field [15]. Resected masses can be imaged on all surfaces for the presence of tumor and the validation of clean tumor margins. Intra-operative imaging could eliminate the time spent in the surgical pathology lab when a fully-staffed operating room is waiting for pathological diagnoses of tissue specimens. Fourth, following resection of tumor masses, OCT can be used to scan the walls of the tumor cavity for the presence of residual tumor or metastasizing tumor cells that have extended beyond the surgical tumor margin.

The use of high-resolution imaging of tumor morphology and individual cells may potentially represent a new paradigm of surgical treatment. Surgical procedures in the past have routinely been performed at the macroscopic scale in the operating room, relying on histological observations in the surgical pathology suite to confirm or exclude the presence of abnormal tumor cells along tumor margins or within tissue specimens. The high-resolution, real-time imaging capabilities of OCT may enable these histopathological observations and diagnoses to be made intra-operatively in real-time. Undoubtedly this will be more cost efficient in terms of dollars and time.

This paper has provided a brief overview of the OCT technology along with OCT images and corresponding histopathological observations to validate the feasibility and potential for this technology in the investigation and treatment of breast cancer. Future studies will use this technology to address specific research questions and to perform intra-operative image-guided procedures. The long-term benefit of OCT will be to enhance visualization for understanding disease processes, pharmacotherapeutic interventions, and surgical options in the treatment of breast cancer.

Acknowledgements

We thank Dr Tapas DasGupta, Department Head of Surgical Oncology at the University of Illinois-Chicago Medial Center, for his helpful discussions and contributions and Dr Amy Oldenburg from the Beckman Institute for her technical assistance in operating our OCT system. This research was supported by grants from the National Institutes of Health (NCI, NIBIB) (R01 EB00108-1), the National Aeronautics and Space Administration (NAS2-02057), the Whitaker Foundation, and the University of Illinois Intercampus Research Initiative in Biotechnology. Additional information can be found at <http://nb.beckman.uiuc.edu/biophotonics>.

References

1. American Cancer Society, Cancer Facts & Figures, 2003
2. American Cancer Society, Cancer Prevention & Early Detection Facts & Figures, 2003
3. Profio AE, Doiron DR: Transport of light in tissue in photodynamic therapy of cancer. *Photochem Photobiol* 46: 591–599, 1987
4. Yodh AG, Chance B: Spectroscopy and imaging with diffusing light. *Phys Today* 48: 34–40, 1995
5. Jiang H, Xu Y, Iftimia N, Eggert J, Klove K, Baron L, Fajardo L: Three-dimensional optical tomographic imaging of breast in a human subject. *IEEE Trans Med Imaging* 20: 1334–1340, 2001
6. Shah N, Cerussi A, Eker C, Espinoza J, Butler J, Fishkin J, Hornung R, Tromberg B: Noninvasive functional optical spectroscopy of human breast tissue. *Proc Natl Acad Sci USA* 98: 4420–4425, 2001
7. Huang D, Swanson EA, Lin CP, Schuman JS, Stinson WG, Chang W, Hee MR, Flotte T, Gregory K, Puliafito CA, Fujimoto JG: Optical coherence tomography. *Science* 254: 1178–1181, 1991
8. Bouma BE, Tearney GJ (eds): *Handbook of Optical Coherence Tomography*. Marcel Dekker, New York, NY, 2002
9. Boppart SA, Bouma BE, Pitris C, Tearney GJ, Southern JF, Brezinski ME, Fujimoto JG: Intraoperative assessment of microsurgery with three-dimensional optical coherence tomography. *Radiology* 208: 81–86, 1998
10. Povazay B, Bizheva K, Unterhuber A, Hermann B, Sallmann H, Fercher AF, Drexler W, Apolonski A, Wadsworth WJ, Knight JC, Russell PSJ, Vetterlein M, Scherzer E: Submicrometer axial resolution optical coherence tomography. *Opt Lett* 27: 1800–1802, 2002
11. Tearney GJ, Brezinski ME, Bouma BE, Boppart SA, Pitris C, Southern JF, Fujimoto JG: *In vivo* endoscopic optical biopsy with optical coherence tomography. *Science* 276: 2037–2039, 1997
12. Sergeev AM, Gelikonov VM, Gelikonov GV, Feldchtein FI, Kuranov RV, Gladkova ND, Shakhova NM, Snopova LB, Shakov AV, Kuznetsova IA, Denisenko AN, Pochinko VV, Chumakov YP, Streltsova OS: *In vivo* endoscopic OCT imaging of precancer and cancer states of human mucosa. *Opt Express* 1: 432–440, 1997
13. Boppart SA, Brezinski ME, Pitris C, Fujimoto JG: Optical coherence tomography for neurosurgical imaging of human intracortical melanoma. *Neurosurgery* 43: 834–841, 1998
14. Li X, Chudoba C, Ko T, Pitris C, Fujimoto JG: Imaging needle for optical coherence tomography. *Opt Lett* 25: 1520–1522, 2000
15. Boppart SA, Bouma BE, Pitris C, Tearney GJ, Fujimoto JG: Forward-imaging instruments for optical coherence tomography. *Opt Lett* 22: 1618–1620, 1997
16. Holland R, Veling SH, Mravunac M, Hendriks JH: Histologic multifocality of T1S, T1–T2 breast carcinomas. Implications for clinical trials of breast-conserving surgery. *Cancer* 56: 979–990, 1985
17. Katz A, Strom EA, Buchholz TA, Thames HD, Smith CD, Jhingran A, Hortobagyi G, Buzdar AU, Theriault R, Singletary SE, McNeese MD: Locoregional recurrence patterns after mastectomy and doxorubicin-based chemotherapy: implications for postoperative irradiation. *J Clin Oncol* 18: 2817–2827, 2000
18. Schneebaum S, Even-Sapir E, Cohen M, Shacham-Lehrman H, Gat A, Brazovsky E, Livshitz G, Stadler J, Skornick Y: Clinical applications of gamma-detection probes – radioguided surgery. *Eur J Nucl Med* 26: S26–S35, 1999
19. Kaplan I, Oldenburg NE, Meskill P, Blake M, Church P, Holupka EJ: Real time MRI-ultrasound image guided stereotactic prostate biopsy. *Magn Reson Imaging* 20: 295–299, 2002
20. Puliafito CA, Hee MR, Schuman JS, Fujimoto JG: *Optical Coherence Tomography of Ocular Diseases*. Slack Inc., Thorofare, NJ, 1995

21. Schmitt JM, Knuttel A, Yadlowsky M, Eckhaus AA: Optical coherence tomography of a dense tissue: statistics of attenuation and backscattering. *Phys Med Biol* 39: 1705–1720, 1994
22. Schmitt JM, Yadlowsky MJ, Bonner RF: Subsurface imaging of living skin with optical coherence microscopy. *Dermatology* 191: 93–98, 1995
23. Brezinski ME, Tearney GJ, Bouma BE, Izatt JA, Hee MR, Swanson EA, Southern JF, Fujimoto JG: Optical coherence tomography for optical biopsy: properties and demonstration of vascular pathology. *Circulation* 93: 1206–1213, 1996
24. Tearney GJ, Brezinski ME, Southern JF, Bouma BE, Boppart SA, Fujimoto JG: Optical biopsy in human gastrointestinal tissue using optical coherence tomography. *Am J Gastroenterol* 92: 1800–1804, 1997
25. Tearney GJ, Brezinski ME, Southern JF, Bouma BE, Boppart SA, Fujimoto JG: Optical biopsy in human urologic tissue using optical coherence tomography. *J Urol* 157: 1915–1919, 1997
26. Bouma BE, Tearney GJ, Boppart SA, Hee MR, Brezinski ME, Fujimoto JG: High resolution optical coherence tomographic imaging using a modelocked Ti:Al₂O₃ laser. *Opt Lett* 20: 1486–1488, 1995
27. Drexler W, Morgner U, Kartner FX, Pitris C, Boppart SA, Li X, Ippen EP, Fujimoto JG: *In vivo* ultrahigh resolution optical coherence tomography. *Opt Lett* 24: 1221–1223, 1999
28. Tearney GJ, Bouma BE, Boppart SA, Golubovic B, Swanson EA, Fujimoto JG: Rapid acquisition of *in vivo* biological images using optical coherence tomography. *Opt Lett* 21: 1408–1410, 1996
29. Ren H, Brecke KM, Ding Z, Zhao Y, Nelson JS, Chen Z: Imaging and quantifying transverse flow velocity with the Doppler bandwidth in a phase-resolved functional optical coherence tomography. *Opt Lett* 27: 409–411, 2002
30. Yazdanfar S, Izatt JA: Self-referenced Doppler optical coherence tomography. *Opt Lett* 27: 2085–2087, 2002
31. Pierce MC, Park BH, Cense B, de Boer JF: Simultaneous intensity, birefringence, and flow measurements with high-speed fiber-based optical coherence tomography. *Opt Lett* 27: 1534–1536, 2002
32. Tearney GJ, Boppart SA, Bouma BE, Brezinski ME, Weissman NJ, Southern JF, Fujimoto JG: Scanning single-mode fiber optic catheter-endoscope for optical coherence tomography. *Opt Lett* 21: 1–3, 1996
33. Pan Y, Xie H, Fedder GK: Endoscopic optical coherence tomography based on a microelectromechanical mirror. *Opt Lett* 26: 1966–1968, 2001
34. Bouma BE, Tearney GJ, Compton CC, Nishioka NS: High-resolution imaging of the human esophagus and stomach *in vivo* using optical coherence tomography. *Gastrointest Endosc* 51: 467–474, 2000
35. Sivak MV Jr, Kobayashi K, Izatt JA, Rollins AM, Ung-Runyawee R, Chak A, Wong RC, Isenberg GA, Willis J: High-resolution endoscopic imaging of the gastrointestinal tract using optical coherence tomography. *Gastrointest Endosc* 51: 474–479, 2000
36. Li X, Boppart SA, Van Dam J, Mashimo H, Mutinga M, Drexler W, Klein M, Pitris C, Krinsky ML, Brezinski ME, Fujimoto JG: Optical coherence tomography: advanced technology for the endoscopic imaging of Barrett's esophagus. *Endoscopy* 32: 921–930, 2000
37. Jang IK, Bouma BE, Kang DH, Park SJ, Park SW, Seung KB, Choi KB, Shishkov M, Schlendorf K, Pomerantsev E, Houser SL, Aretz HT, Tearney GJ: Visualization of coronary atherosclerotic plaques in patients using optical coherence tomography: comparison with intravascular ultrasound. *J Am Coll Cardiol* 39: 604–609, 2002
38. Pitris C, Goodman AK, Boppart SA, Libis JJ, Fujimoto JG, Brezinski ME: High resolution imaging of gynecological neoplasms using optical coherence tomography. *Obstet Gynecol* 93: 135–139, 1999
39. Pitris C, Jesser C, Boppart SA, Stamper D, Brezinski ME, Fujimoto JG: Feasibility of optical coherence tomography for high resolution imaging of human gastrointestinal tract malignancies. *J Gastroenterol* 35: 87–92, 1999
40. Xie TQ, Zeidel ML, Pan Y: Detection of tumorigenesis in urinary bladder with optical coherence tomography: optical characterization of morphological changes. *Opt Express* 10: 1431–1443, 2002
41. Boppart SA, Brezinski ME, Bouma BE, Tearney GJ, Fujimoto JG: Investigation of developing embryonic morphology using optical coherence tomography. *Dev Biol* 177: 54–63, 1996
42. Boppart SA, Tearney GJ, Bouma BE, Southern JF, Brezinski ME, Fujimoto JG: Noninvasive assessment of the developing *Xenopus* cardiovascular system using optical coherence tomography. *Proc Natl Acad Sci USA* 94: 4256–4261, 1997
43. Boppart SA, Bouma BE, Pitris C, Southern JF, Brezinski ME, Fujimoto JG: *In vivo* cellular optical coherence tomography imaging. *Nature Med* 4: 861–864, 1998
44. Brezinski ME, Tearney GJ, Boppart SA, Swanson EA, Southern JF, Fujimoto JG: Optical biopsy with optical coherence tomography: feasibility for surgical diagnostics. *J Surg Res* 71: 32–40, 1997
45. Boppart SA, Herrmann JM, Pitris C, Stamper DL, Brezinski ME, Fujimoto JG: High-resolution optical coherence tomography guided laser ablation of surgical tissue. *J Surg Res* 82: 275–284, 1999
46. Boppart SA, Goodman AK, Pitris C, Jesser C, Libis JJ, Brezinski ME, Fujimoto JG: High-resolution imaging of endometriosis and ovarian carcinoma with optical coherence tomography: feasibility for laparoscopic-based imaging. *Br J Obstet Gyn* 106: 1071–1077, 1999
47. Boppart SA, Herrmann JM, Pitris C, Stamper DL, Brezinski ME, Fujimoto JG: Real-time optical coherence tomography for minimally-invasive imaging of prostate ablation. *Comp Aided Surg* 6: 94–103, 2001
48. Russo J, Russo I, van Zwieten M, Rogers A, Gusterson B: Classification of neoplastic and non-neoplastic lesions of the rat mammary gland. In: Jones T, Mohr U, Hunt R (eds) *Integument and Mammary Glands, Monographs on Pathology of Laboratory Animals*. Springer-Verlag, Berlin, 1989, pp 275–340
49. McCormick D, Adamowski C, Fiks A, Moon R: Lifetime dose–response relationships for mammary tumors induction by a single administration of *N*-methyl-*N*-nitrosourea. *Cancer Res* 41: 1690–1694, 1981
50. Gullino P, Pettigrew H, Grantham F: *N*-nitrosomethylurea as mammary gland carcinogen in rats. *J Natl Cancer Inst* 54: 401–409, 1975
51. Tseng M: Ultrastructure of the hormone-dependent *N*-nitrosomethylurea-induced mammary carcinoma of the rat. *Cancer Res* 40: 3112–3115, 1980
52. Arafah B, Finegan H, Roe J, Manni A, Pearson O: Hormone dependency in *N*-nitrosomethylurea-induced rat mammary tumors. *Endocrinology* 111: 584–588, 1982
53. Bigsby R: Synergistic tumor promoter effects of estrone and progesterone in methylnitrosourea-induced rat mammary cancer. *Cancer Lett* 179: 113–110, 2001

54. Thompson H, McGinley J, Knott K, Spoelstra N, Wolfe P: Vascular density profile of rat mammary carcinomas induced by 1-methyl-1-nitrosourea: implications for the investigation of angiogenesis. *Carcinogenesis* 23: 847–854, 2002
55. Dulbecco R, Armstrong B, Allen W, Bowman M: Distribution of developmental markers in rat mammary tumors induced by *N*-nitrosomethylurea. *Cancer Res* 46: 5144–5152, 1986
56. Anderson C, Beattie C: Cellular kinetics of rat mammary gland terminal end bud epithelium exposed to *N*-methyl-*N*-nitrosomethylurea *in vivo*. *Cancer Res* 52: 5076–5081, 1992
57. Singh M, McGinley J, Thompson H: A comparison of the histopathology of premalignant and malignant mammary gland lesions induced in sexually immature rats with those occurring in the human. *Lab Invest* 80: 221–231, 2000
58. Jin Z, Houle B, Mikheev A, Cha R, Zarbl H: Alterations in H-ras 1 promoter conformation during *N*-nitroso-*N*-methylurea-induced mammary carcinogenesis and pregnancy. *Cancer Res* 56: 4927–4935, 1996
59. Thompson H, McGinley J, Rothhammer K, Singh M: Ovarian hormone dependence of premalignant and malignant mammary gland lesions induced in pre-pubertal rats by 1-methyl-1-nitrosourea. *Carcinogenesis* 19: 383–386, 1998
60. Lu J, Jiang C, Mitrenga T, Cutter G, Thompson H: Pathogenetic characterization of 1-methyl-1-nitrosourea-induced mammary carcinomas in the rat. *Carcinogenesis* 19: 223–227, 1998
61. Thompson H, Adlaka H, Singh M: Effect of carcinogen dose and age at administration on induction of mammary carcinogenesis by 1-methyl-1-nitrosourea. *Carcinogenesis* 13: 1535–1539, 1992
62. Thompson H, Adlaka H: Dose-responsive induction of mammary gland carcinomas by the intraperitoneal injection of 1-methyl-1-nitrosourea. *Cancer Res* 51: 3411–3415, 1991
63. Thompson H, McGinley J, Rothhammer K, Singh M: Rapid induction of mammary intraductal proliferations, ductal carcinoma *in situ* and carcinomas by the injection of sexually immature female rats with 1-methyl-1-nitrosourea. *Carcinogenesis* 16: 2407–2411, 1995
64. Thordarson G, Lee AV, McCarty M, Van Horn K, Chu O, Chou Y-C, Yang J, Guzman RC, Nandi S, Talamantes F: Growth and characterization of *N*-methyl-*N*-nitrosourea-induced mammary tumors in intact and ovariectomized rats. *Carcinogenesis* 22: 2039–2047, 2001
65. Rose D, Fischer A, Jordan G: Activity of the antiestrogen tamoxifen against *N*-nitrosomethylurea-induced rat mammary carcinomas. *Eur J Cancer* 17: 893–898, 1981
66. Green A, Skilkaitis A, Christov K: 4-(hydroxyphenyl) retinamide selectively inhibits the development and progression of the ductal hyperplastic lesions and carcinoma *in situ* in mammary gland. *Carcinogenesis* 20: 1535–1540, 1999
67. Crist K, Chaudhuri B, Shivaram S, Chaudhuri PK: Ductal carcinoma *in situ* in rat's mammary gland. *J Surg Res* 52: 205–208, 1992
68. Thompson HJ, Singh M, McGinley J: Classification of premalignant and malignant lesions developing in the rat mammary gland after injection of sexually immature rats with 1-methyl-1-nitrosourea. *J Mammary Gland Biol Neoplasia* 5: 201–210, 2000
69. Thompson HJ, Singh M: Rat models of premalignant breast disease. *J Mammary Gland Biol Neoplasia* 5: 409–420, 2000
70. Sivaraman L, Gay J, Hilsenbeck SG, Shine HD, Conneely OM, Medina D, O'Malley BW: Effect of selective ablation of proliferating mammary epithelial cells on MNU induced rat mammary tumorigenesis. *Breast Cancer Res Treat* 73: 75–83, 2002
71. Marks DL, Oldenburg AL, Reynolds JJ, Boppart SA: Study of an ultrahigh numerical aperture fiber continuum generation source for optical coherence tomography. *Opt Lett* 27: 2010–2012, 2002
72. Oldenburg AL, Reynolds JJ, Marks DL, Boppart SA: Fast-Fourier-domain delay line for *in vivo* optical coherence tomography with a polygonal scanner. *Appl Opt* 42: 4606–4611, 2003
73. Marks DL, Oldenburg AL, Reynolds JJ, Boppart SA: Autofocus algorithm for dispersion correction in optical coherence tomography. *Appl Opt* 42: 3038–3046, 2003
74. Lee TM, Oldenburg AL, Sitafalwalla S, Marks DL, Luo W, Toublan FJJ, Suslick KS, Boppart SA: Engineered microsphere contrast agents for optical coherence tomography. *Opt Lett* 28: 1546–1548, 2003
75. Toth CA, Birngruber R, Boppart SA, Hee MR, Fujimoto JG, DiCarlo CD, Swanson EA, Cain CP, Narayan DG, Noojin GD, Roach WP: Argon laser retinal lesions evaluated *in vivo* by optical coherence tomography. *Am J Ophthalmol* 123: 188–198, 1997
76. Toth CA, Narayan DG, Boppart SA, Hee MR, Fujimoto JG, Birngruber R, Cain CP, DiCarlo CD, Roach WP: A comparison of retinal morphology viewed by optical coherence tomography and by light microscopy. *Arch Ophthalmol* 115: 1425–1428, 1997

Address for offprints and correspondence: Stephen A. Boppart, MD, PhD, Beckman Institute for Advanced Science and Technology, 405 N. Mathews Avenue, Urbana, IL 61801, USA; *Tel.:* +1-217-244-7479; *Fax:* +1-217-244-1995; *E-mail:* boppart@uiuc.edu